Enantiomerically Pure Chiral Coordination Polymers: Synthesis, Spectroscopy, and Electrochemistry in Solution and on Surfaces

Stefan Bernhard,[†] Kazutake Takada,[†] Diego J. Díaz,[†] Héctor D. Abruña,*[,†] and Hansruedi Mürner[‡]

Contribution from the Department of Chemistry and Chemical Biology, Baker Laboratory, Cornell University, Ithaca, New York 14853-1301, and Institut de Chimie Minérale et Analytique, Université de Lausanne-BCH, CH-1015 Lausanne, Switzerland

Received April 23, 2001. Revised Manuscript Received August 3, 2001

Abstract: The two enantiomerically pure bridging ligands (±)-[**ctpy-x-ctpy**] have been prepared employing a two-fold stereospecific alkylation reaction of the enantiomerically pure, chiral terpyridyl-type ligands (±)-**ctpy**. The reaction of each of the enantiomerically pure bridging ligands with Fe^{2+} gives rise to chiral coordination polymers whose formation and stoichiometry were followed spectrophotometrically. An assignment of the absolute configuration of the formed helical polymeric structures was carried out on the basis of circular dichroism studies. Highly ordered domains (as determined from STM imaging) of the enantiomerically pure chiral redox polymers could be prepared via the interfacial reaction, over an HOPG substrate, of the bridging ligand in CH_2Cl_2 and $FeSO_4$ in water. The degree of polymerization was estimated to be up to 60 from analysis of the STM images of the highly ordered domains on HOPG. The helicality of the domains was compared to the configuration obtained from the circular dichroism studies. The electrochemical properties of the polymers were investigated using cyclic voltammetry and the results compared to those of the respective monomeric complexes. The redox behavior of the iron centers in the polymer was comparable to that of the monomeric complex $[Fe((-)\text{-}\mathbf{ctpy})_2](PF_6)_2$ as well as to that of $[Fe(tpy)_2](PF_6)_2$. The polymeric materials undergo electrodeposition following the two-electron reduction of each bridging ligand unit (one electron per terpyridine group). No ligand-mediated metal−metal interactions were evident from the cyclic voltammetric measurements, suggesting that the metal centers act independently. Moreover, oxidation of the metal centers within the polymeric materials did not give rise to electrodeposition.

Introduction

Recently there has been, and continues to be, a widespread interest in the preparation of chiral ligand systems for the coordination of transition metals due to their application in preparative catalytic reactions and the interesting electrochemical, photophysical, and photochemical properties of the resulting complexes.[1] To date, optically pure ligands have been prepared by the separation of the respective enantiomers through diastereomers or by their preparation from optically pure precursors.[2] Von Zelewsky and co-workers employed the latter strategy in pioneering the ability to control the helical chirality around metal centers through the use of chiral terpene building blocks.[3] A similar strategy was later used by Thummel et al. for the synthesis of chiral 1,10-phenanthroline ligands for the preparation of chiral rhodium complexes, which were then employed in stereoselective electrosynthetic reactions.[4] Whereas the above-mentioned work deals with the preparation of molecular chiral complexes, to our knowledge, little work has been devoted to the development of chiral, transition metal coordination polymers.[5] The interest in coordination metal polymers arises from their potential application in electronic, magnetic, and optical devices.[6] The ability to prepare coordination polymers has evolved as a result of the experience gained from studies on mononuclear coordination compounds over the past decades. The unique photophysical and photochemical properties of ruthenium(II)−tris(diimine) compounds stimulated the preparation of ruthenium-based photoactive polymers based on 2,2′-bipyridine and terpyridine bridging ligands, with the photoconducting properties of one of the polymers being studied and reported by Ng and Chan.[7] Similar studies were performed with bridging ligands containing 2,9-disubstituted 1,10-phenanthrolines capable of coordinating with a tetrahedral geometry to copper(I) and silver(I) ions.[8] Elliott and co-workers employed Co(II)- and Fe(II)-based terpyridine polymers to investigate the

[†] Cornell University.

[‡] Université de Lausanne-BCH.

(1) (a) Keene, F. R. *Coord. Chem. Rev.* **1997**, *166*, 121−151. (b) Von Zelewsky, A. *Stereochemistry of Coordination Compounds*; John Wiley & Sons Ltd.: New York, 1996.

(2) (a) Gladiali, S.; Pinna, L.; Delogu, G.; de Stefano, M.; Zassinovich, G.; Mestroni, G. *Tetrahedron: Asymmetry* **1990**, *1*, 635−648. (b) Von Zelewsky, A.; Mamula, O. *J. Chem. Soc., Dalton Trans.* **2000**, 219. (c) Knof, U.; von Zelewsky, A. *Angew. Chem., Int. Ed.* **1999**, *38*, 302−322.

(3) (a) Hayoz, P.; Von Zelewsky, A.; Stoeckli-Evans, H. *J. Am. Chem. Soc.* **1993**, *115*, 5111−14. (b) Muerner, H.; Belser, P.; von Zelewsky, A. *J. Am. Chem. Soc.* **1996**, *118*, 7989.

(4) Moutet, J.-C.; Cho, L. Y.; Duboc-Toia, C.; Ménage, S.; Riesgo, E. C.; Thummel, R. P. *New J. Chem.* **1999**, *23*, 939−944.

(5) Chen, J.; MacDonnell, F. M. *Chem. Commun.* **1999**, 2529−2530.

(6) (a) Collier, C. P.; Matterstei, G.; Wong, E. W.; Luo, Y.; Beverly, K.; Sampaio, J.; Raymo, F. M.; Stoddart, J. F.; Heath, J. R. *Science* **2000**, *289*, 1172−1175. (b) Bergstedt, T. S.; Hauser, B. T.; Schanze, K. S. *J. Am. Chem. Soc.* **1994**, *116*, 8380−8381. (c) Ohkoshi, S.-I.; Fujishima, A.; Hashimoto, K. *J. Am. Chem. Soc.* **1998**, *120*, 5349−5350.

(7) Ng, W. Y.; Chan, W. K. *Adv. Mater.* **1997**, *9*, 716−719.

(8) (a) Velten, U.; Lahn, B.; Rehahn, M. *Macromol. Chem. Phys.* **1997**, *198*, 2789−2816. (b) Velten, U.; Rehahn, M. *Macromol. Chem. Phys.* **1998**, *199*, 127−140. (c) Velten, U.; Rehahn, M. *Chem. Commun.* **1996**, 2639−2640.

10.1021/ja011020j CCC: $20.00
Published on Web 10/02/2001

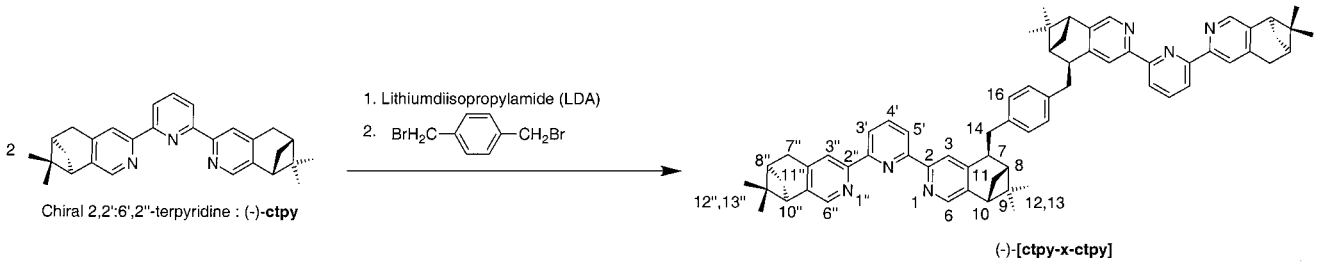

Figure 1. Synthetic pathway for the preparation of the chiral bridging ligand (−)-**[ctpy-x-ctpy]**. The (+)-**[ctpy-x-ctpy]** enantiomer was prepared starting from (1*S*)-(+)-myrtenal.

mechanism of the electrocatalytic reduction of O_2 and CO_2.[9] In addition, the preparation of coordination polymers via electropolymerizable ligands such as vinyl-2,2′-bipyridines and related materials is now well established. A vast collection of materials has been prepared and characterized using this approach, and a number of electronic, electrocatalytic, electroluminescent, and photovoltaic applications have been explored.[10] More recently, Fe(II) polymers have been synthesized using rigid and more symmetrical bridging ligands; they could be subsequently immobilized as films on electrode surfaces exhibiting interesting spectroelectrochemical properties.[11]

In an effort to combine the properties of coordination polymers and chiral ligand systems, we report herein on the synthesis and characterization of the pure, chiral enantiomers of a 2,2′:6′,2″-terpyridine bridging ligand (±)-[**ctpy-x-ctpy**] (Figure 1). The Fe(II) coordination polymers of both (pure) enantiomers were subsequently prepared and their electrochemical and spectroscopic properties explored using cyclic voltammetry, the electrochemical quartz crystal microbalance (including admittance measurements), UV−vis spectroscopy, and circular dichroism. In addition, highly ordered arrays on HOPG, which were imaged via STM, of these chiral redox polymers could be prepared through an interfacial reaction technique.

Experimental Section

General. Solvents and reagents for synthesis were purchased from Aldrich and used without further purification. (1*R*)-(−)-Myrtenal for the preparation of (−)-**ctpy** was obtained from Fluka. Acetonitrile (AN) and dichloromethane (Burdick and Jackson; distilled in glass) for electrochemical experiments were dried over 4 Å molecular sieves for at least 48 h. Tetra-*n*-butylammonium hexafluorophosphate (TBAH) (GFS Chemicals) was recrystallized three times from ethyl acetate and dried under vacuum for 96 h. ESI-MS spectra were obtained either on a Micromass Quattro1 triple-quadrupole tamdem mass spectrometer or a Micromass Autospec high-resolution mass spectrometer. A Varian Inova-400 spectrometer was used to collect ^{1}H and ^{13}C NMR data. The specific rotation of the ligands was determined with a Perkin-Elmer 241 polarimeter.

UV−Vis and CD Spectroscopic Measurements. UV−vis spectra were recorded using a Hewlett-Packard 8453 diode-array spectrometer. A 100 mL amount of a 10 μM solution of (−)-**[ctpy-x-ctpy]** in chloroform was titrated with an $Fe(BF_4)_2$ solution (5.0 mg/10 mL methanol, 1.48 mM), and the UV−vis spectra were measured in a 1 cm quartz cell.

Circular dichroism spectra (CD) were recorded in 1 cm quartz cells at 20 °C on a Jobin Yvon CD 6 spectrometer. In a typical titration experiment, aliquots of $Fe(BF_4)_2$ (0.978 mM in dry MeOH) were added with a micropipet to a solution of pure (−)-**[ctpy-x-ctpy]** or (+)-**[ctpy-x-ctpy]** in dry $CHCl_3$ (50 mL, 10 μM). The CD spectra were taken after 5 min of vigorous mixing and were later corrected for dilution. CD spectra in the visible region were recorded for 10× more concentrated samples. These were obtained after evaporation of solutions containing 1.5 equiv of Fe(II) per ligand molecule under nitrogen and redissolving in 5.0 mL of $CHCl_3$/MeOH (9:1).

Electrochemical Measurements. Electrochemical experiments were carried out with a BAS CV-27 potentiostat. Three-compartment electrochemical cells (separated by medium-porosity sintered glass disks) with the provision for gas addition were employed. All joints were standard taper so that all compartments could be hermetically sealed with Teflon adapters. A platinum disk (geometric area = 0.008 cm^2) was used as a working electrode. The electrode was polished prior to use with 1 μm diamond paste (Buehler) and rinsed thoroughly with water and acetone. A large area platinum wire coil was used as a counter electrode. All potentials are referenced to a saturated Ag/AgCl electrode without regard for the liquid junction potential. Instrumentation for electrochemical quartz microbalance (EQCM) has been described previously.[12] The basis for this technique employing a quartz crystal resonator is the Sauerbrey equation,[13]

$$\Delta m = -C_f \Delta f \qquad (1)$$

where Δm (g cm^{-2}) is the total change in mass, C_f (g Hz^{-1} cm^{-2}) is a proportionality constant for an AT-cut quartz crystal resonator, and Δf (Hz) is the change in frequency.

STM Imaging. Films were prepared by bringing into contact a 10 μM solution of (−)-**[ctpy-x-ctpy]** or (+)-**[ctpy-x-ctpy]** in CH_2Cl_2 with aqueous $FeSO_4$ (0.01 M) over the surface of a freshly cleaved HOPG substrate (ZYA Grade, Union Carbide). The reaction was allowed to proceed at room temperature for 24 h. The surface was then thoroughly rinsed with H_2O and CH_2Cl_2 to remove excess reactants.

STM images were obtained in air using a Molecular Imaging 10 μm scanner, Molecular Imaging isolation chamber, and Digital Instruments Nanoscope E controller. Electrochemically etched Pt/Ir (80:20) tips were used for all STM measurements. All images shown are unfiltered, taken on-line, and no off-line zoom was used. Bias voltages between +500 and +1000 mV and setpoint currents between 1.0 and 1.6 nA were employed. The scan rates were between 4 Hz for the larger scale images and 10 Hz for the smaller size images. The images are taken at 512 samples resolution to obtain better detailed images.

Synthesis. (±)-[ctpy-x-ctpy]. A solution of the chiral terpyridine (−)-**ctpy**[14] (0.50 g, 1.19 mmol) in 25 mL of dry THF was cooled to −40 °C, and a solution of lithium diisopropylamide (0.6 mL, 2 M, 1.2 mmol) was added through a syringe under nitrogen. The deep blue solution was allowed to warm to −5 °C and kept at this temperature for 1 h. After the reaction mixture was cooled to −20 °C, α,α′-dibromo-*p*-xylene (0.10 g, 0.38 mmol) was added, and the mixture was then left to warm to room temperature. After 4 h the blue mixture was

(9) Feldheim, D. L.; Baldy, C. J.; Sebring, P.; Hendrickson, S. M.; Elliott, C. M. *J. Electrochem. Soc.* **1995**, *142*, 3366−3372.

(10) (a) Abruña, H. D.; Denisevich, P.; Umaña, M.; Meyer, T. J.; Murray, R. W. *J. Am. Chem. Soc.* **1981**, *103*, 1−5. (b) Denisevich, P.; Abruña, H. D.; Leidner, C. R.; Meyer, T. J.; Murray, R. W. *Inorg. Chem.* **1982**, *21*, 2153-2161. (c) Bommarito, S. L.; Lowery-Bretz, S. P.; Abruña, H. D. *Inorg. Chem.* **1992**, *31*, 495−501.

(11) Kimura, M.; Horai, T.; Muto, T.; Hanabusa, K.; Shirai, H. *Chem. Lett.* **1999**, 1129−1130.

(12) Takada, K.; Storrier, G. D.; Pariente, F.; Abruña, H. D. *J. Phys. Chem. B* **1998**, *102*, 1387−1396.

(13) Sauerbrey, G. *Z. Phys.* **1959**, *155*, 206−222.

(14) Ziegler, M.; Monney, V.; Stoeckli-Evans, H.; Von Zelewsky, A.; Sasaki, I.; Dupic, G.; Daran, J.-C.; Balavoine, G. A *J. Chem. Soc. Dalton Trans.* **1999**, 667−675.

quenched with ammonium chloride solution (100 mL, 5%) and extracted with CH_2Cl_2 (3 × 100 mL). The combined organic layers were washed with water (100 mL and dried with $MgSO_4$, and the solvent was removed under reduced pressure. To separate the (−)-**ctpy** from the product, the residue, a yellow powder, was dissolved in 20 mL of CH_2Cl_2, and 20 mL of hexane was added. Slow evaporation of the CH_2Cl_2 at 0 °C led to the crystallization of a white solid, which was separated by filtration. Repetition of this crystallization procedure and flash chromatography (CH_2Cl_2/neutral alumina) yielded a white solid (−)-**[ctpy-x-ctpy]** (0.21 g, 0.22 mmol, 58%). Analytical data: ^{1}H NMR ($CDCl_3$, 400 MHz) δ 8.57 (2H, s, H(3)), 8.36 (1H, d, $J^3(H^{5'}H^{4'}) = 7.9$, H(5′)), 8.35 (1H, d, $J^3(H^{3'}H^{4'}) = 7.9$, H(3′)), 8.35 (2H, s, H(3″)), 8.25 (2H, s, H(6)), 8.21 (2H, s, H(6″)), 7.92 (1H, dd, $J^3(H^{4'}H^{3'}) = 7.9$, $J^3(H^{4'}H^{5'}) = 7.9$, H(4′)), 7.24 (4H, s, H(16)), 3.51 (2H, dd, $J^3(H^{14a}H^7) = 13.8$, $J^2(H^{14a}H^{14b}) = 3.8$, H(14a)), 3.39 (2H, d, $J^3(H^{14b}H^7) = 11.8$, H(14b)), 3.11 (4H,m, H(7″)), 2.90 (2H, dd, $J^3(H^{10}H^{11a}) = 5.2$, $J^3(H^{10}H^{11b}) = 5.2$, H(10)), 2.87 (2H, dd, $J^3(H^{10''}H^{11a''}) = 5.2$, $J^3(H^{10''}H^{11b''}) = 5.2$, H(10″)), 2.78 (2H, dd, $J^3(H^7H^{14a}) = 13.7$, $J^3(H^7H^{14a}) = 11.3$, H(7)), 2.70 (2H, ddd, $J^3(H^{11b''}H^{11a''}) = 9.7$, $J^3(H^{11b''}H^{10''}) = 5.6$, $J^3(H^{11b''}H^{8''}) = 5.5$, H(11b″)), 2.58 (2H, ddd, $J^3(H^{11b}H^{11a}) = 9.8$, $J^3(H^{11b}H^{10}) = 5.6$, $J^3(H^{11b}H^8) = 5.5$, H(11b)), 2.31 (2H, m, H(8″)), 2.05 (2H, m, H(8)), 1.41 (2H, d, $J^3(H^{11a}H^{11b}) = 9.8$, H(11a)), 1.39 (6H, s, H(12″)), 1.35 (6H, s, H(12)), 1.23 (2H, d, $J^3(H^{11a''}H^{11b''}) = 9.5$, H(11a″)), 0.65 (6H, s, H(13″)), 0.61 (6H, s, H(13)); ^{13}C NMR ($CDCl_3$, 100 MHz) δ 156.0, 155.9, 155.0, 154.6, 148.7, 145.7, 145.6, 145.3, 143.0, 142.8, 137.9, 137.8, 129.3, 120.7, 120.6, 120.5, 119.6, 45.1, 44.5, 42.8, 42.6, 41.0, 40.1, 39.3, 33.1, 33.0, 31.9, 28.1, 29.3, 26.0, 21.5, 21.1; MS (ESI) 474.2 (100%, [M + 2H$^+$]), 946 (50%, [M + H$^+$]); HR-MS (ESI) calcd for $C_{66}H_{69}N_6$ ([M + H$^+$]) 945.5584, found 945.5590; $[\alpha]_D = -168°$ (25 °C, 10 mg in 10 mL of CH_2Cl_2).

(+)-**[ctpy-x-ctpy]** was synthesized in similar yields from (+)-**ctpy**, which was prepared from (1*S*)-(+)-myrtenal.[15] $[\alpha]_D = +166°$ (25 °C, 10 mg in 10 mL of CH_2Cl_2).

[Fe((−)-ctpy)$_2$](PF$_6$)$_2$. A 13.5 mg amount of anhydrous $FeCl_2$ (107 mmol) and 100 mg of (−)-**ctpy** (0.237 mmol) were dissolved in 40 mL of ethanol. The solution immediately turned purple-red and was stirred overnight. After the addition of 120 mL of water, the excess ligand was removed by extraction with 3 × 50 mL of diethyl ether. The aqueous phase was heated on a water bath, and the [Fe((−)-**ctpy**)$_2$](PF$_6$)$_2$ complex was precipitated through addition of 1 g of NH_4PF_6 in 5 mL of water. After isolation of the purple crystals through filtration, the complex was purified by recrystallization from acetone/ether. Analytical data: yield 204 g (72%); ^{1}H NMR (acetone-d_6, 400 MHz) δ 9.03 (2H, d, $J^3(H^{3'}H^{4'}) = 12.1$, H(3′,5′)), 8.73 (1H, dd, $J^3(H^{4'}H^{3'}) = 12.0$, $J^3(H^{4'}H^{5'}) = 12.0$, H(4′)), 8.54 (2H, s, H(3,3″)), 6.86 (2H, s, H(6,6″)), 3.12 (4H, m, H(7)), 2.51 (2H, ddd, $J^3(H^{11b}H^{11a}) = 9.7$, $J^3(H^{11b}H^{10}) = 5.6$, $J^3(H^{11b}H^8) = 5.5$, H(11b,11b″)), 2.45 (2H, dd, $J^3(H^{10}H^{11a}) = 5.4$, $J^3(H^{10}H^{11b}) = 5.4$, H(10, 10″)), 2.20 (m, 2H), 1.18 (6H, s, H(12,12″)), 0.89 (2H, d, $J^3(H^{11a}H^{11b}) = 11.0$, H(11a,11a″)), 0.17 (6H, s, H(13,13″)); MS (ESI) 449.18 (100%, [M − 2PF$_6$]$^{2+}$), 1043.3 (20%, [M − PF$_6$]$^+$).

((−)-[ctpy-x-ctpy])-{[Fe((−)-[ctpy-x-ctpy])](PF$_6$)$_2$}$_n$. A 47 mg amount of (−)-**[ctpy-x-ctpy]** (49.7 μmol) and 6.3 mg of anhydrous $FeCl_2$ (49.8 μmol) were dissolved in 25 mL of ethanol and stirred overnight. A 75 mL amount of water was added, and the purple-red solution was extracted twice with 30 mL of CH_2Cl_2. The aquous layer was heated to boiling, and 1 g of NH_4PF_6 in 5 mL of water was added to precipitate the polymer as the PF_6 salt. The precipitate was filtered and recrystallized twice from acetone/ether. Analytical data: yield 56 mg (72%); ^{1}H NMR (acetone-d_6, 400 MHz) δ 9.05 (m, 2H, H(3′), H(5′)) 8.83 (bs, 1H, H(4′)) 8.72 (bs, 1H, H(3)), 8.54 (bs, 1H, H(3″)), 7.28−7.12 (m, 2H, H(16)), 7.00−6.83 (m, 2H, H(6), H(6″)), 3.52−3.30 (m, 2H, H(14)), 3.20−3.00 (m, 2H, H(7″)), 2.62 (collapsed t, 1H, H(7)), 2.57−2.30 (bm, 4H, H(10), H(10″), H(11), H(11″)), 2.20 (m, 1H, H(8″), 1.85 (m, 1H, H(8)), 1.18 (bs, 3H, H(12″)), 1.15−1.04 (m, H4, H(12), H(11a)), 0.90 (mt, 1H, H(11a″), 0.16 (bs, 3H, H(13″)), 0.07 (bs, 3H, H(13)); MS (ESI) 500.6 (100%, [({(−)-[ctpy-x-ctpy]}Fe)$_n$]$^{2n+}$), 592 (18%, ([({(−)-[ctpy-x-ctpy]}Fe)$_{4n}$](PF$_6$)$_n$]$^{7n+}$), 629 (20%, ([({(−)-[ctpy-x-ctpy]}Fe)$_{3n}$](PF$_6$)$_n$]$^{5n+}$), 662 (8%, ([({(−)-[ctpy-x-ctpy]}Fe)$_{5n}$](PF$_6$)$_{2n}$]$^{8n+}$),

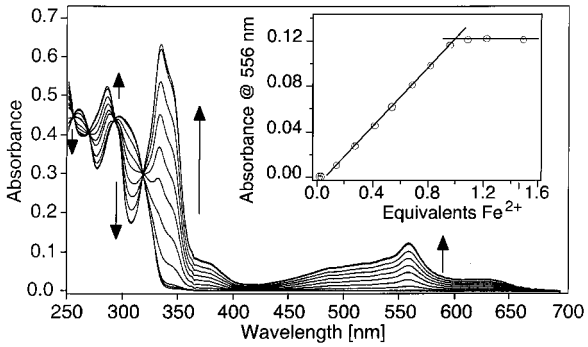

Figure 2. Spectrophotometric titration of (−)-**[ctpy-x-ctpy]** with Fe(BF$_4$)$_2$. The inset shows the absorbance at 556 nm as a function of the Fe(II):(−)-**[ctpy-x-ctpy]** ratio (see Experimental Section for details).

715 (30%, ([({(−)-[ctpy-x-ctpy]}Fe)$_{2n}$](PF$_6$)$_n$]$^{3n+}$), 777 (10%, ([({(−)-[ctpy-x-ctpy]}Fe)$_{5n}$](PF$_6$)$_{3n}$]$^{7n+}$), 823 (12%, ([({(−)-[ctpy-x-ctpy]}Fe)$_{3n}$](PF$_6$)$_n$]$^{4n+}$), 888 (12%, ([({(−)-[ctpy-x-ctpy]}Fe)$_{4n}$](PF$_6$)$_{3n}$]$^{5n+}$), 931 (8%, ([({(−)-[ctpy-x-ctpy]}Fe)$_{5n}$](PF$_6$)$_{4n}$]$^{6n+}$), 961 (7%, ([({(−)-[ctpy-x-ctpy]}Fe)$_{6n}$](PF$_6$)$_{5n}$]$^{7n+}$), 973 (10%, [({(−)-[ctpy-x-ctpy]}$_2$Fe)$^{2+}$]), 1002 (5%, ([({(−)-[ctpy-x-ctpy]}Fe)$_{8n}$](PF$_6$)$_{9n}$]$^{7n+}$), 1020 (1%, [({(−)-[ctpy-x-ctpy]}Fe)](PF$_6$)$_1$−PF$_5$]$^+$),1146 (19%, ([({(−)-[ctpy-x-ctpy]}Fe)$_n$](PF$_6$)$_n$]$^{n+}$), 1469 (19%, ([({(−)-[ctpy-x-ctpy]}Fe)$_{5n}$](PF$_6$)$_{6n}$]$^{4n+}$), 1576 (2%, ([({(−)-[ctpy-x-ctpy]}Fe)$_{4n}$](PF$_6$)$_{5n}$]$^{3n+}$), 1791 (1%, ([({(−)-[ctpy-x-ctpy]}Fe)$_{3n}$](PF$_6$)$_{2n}$]$^{4n+}$), 2006 (1.5%, ([({(−)-[ctpy-x-ctpy]}Fe)$_{5n}$](PF$_6$)$_{7n}$]$^{3n+}$), 2437 (0.5%, ([({(−)-[ctpy-x-ctpy]}Fe)$_{2n}$](PF$_6$)$_{1n}$]$^{3n+}$).

Results and Discussion

Bridging Ligand Synthesis and Polymerization. The synthesis of both enantiomers of the bridging ligand **[ctpy-x-ctpy]** was performed according to literature procedures for analogous bis-2,2′-bipyridine ligands (Figure 1).[16] Additional purification steps were necessary due to the multiple potential deprotonation sites in the chiral 2,2′:6′,2″-terpyridine (±)-**ctpy**. The ligands were fully characterized via ^{1}H NMR, ^{13}C NMR, HR-MS, UV−vis spectroscopy, and rotation angle measurements. The ^{1}H NMR spectrum clearly showed the presence of two different pinene moieties fused to a pyridine ring. Comparison of the spectra with those of bridged 2,2′-bipyridine derivatives led to the conclusion that the alkylation reaction is stereospecific, as established earlier through NOE experiments.[16] The coordination reaction of (−)-**[ctpy-x-ctpy]** with Fe(II) to give rise to a coordination polymer was monitored through a UV−vis spectrophotometric titration (Figure 2). This experiment clearly showed that the coordination reaches the end point at a 1:1 ratio of Fe(II):(−)-**[ctpy-x-ctpy]**. This result confirms that a ((−)-**[ctpy-x-ctpy]**)−{[Fe((−)-**[ctpy-x-ctpy]**)](PF$_6$)$_2$}$_n$ coordination polymer is produced, since due to steric constraints, it is impossible for both **ctpy** subunits within a single ligand molecule to coordinate to the same Fe(II) center in an octahedral geometry (*OC-6*) (Figure 2). The presence of very well-defined isosbestic points at 318, 293, 269, and 255 nm also indicated that there is a simple equilibrium involved.

Circular Dichroism. Results from the spectrophotometric titrations were corroborated by titrations followed by circular dichroism spectroscopy. As depicted in Figure 3, clear spectral changes are observed upon the addition of Fe(II) aliquots to solutions of the (−)-**[ctpy-x-ctpy]** enantiomer. As is evident from the Job plots (inset, Figure 3), these changes level off once a ratio of 1:1 Fe(II):ligand molecule has been reached, as was the case for the spectrophotometric titration (Figure 2).

(15) Shibuya, K. *Synth. Commun.* **1994**, *24*, 2923−2941.

(16) (a) Mürner, H.; von Zelewsky, A.; Stoeckli-Evans, H. *Inorg. Chem.* **1996**, *35*, 3931−3935. (b) Hayoz, P.; Von Zelewsky, A. *Tetrahedron Lett.* **1992**, *33*, 5165−5168.

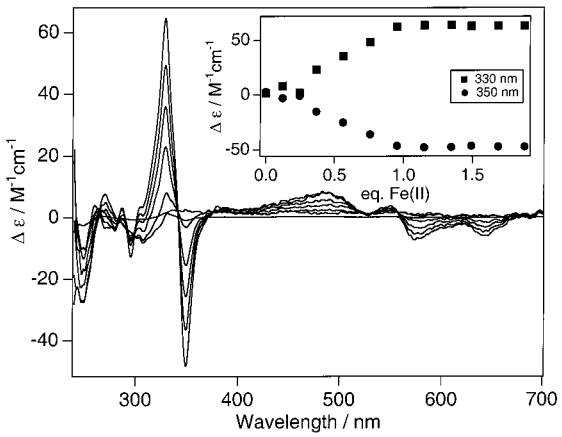

Figure 3. (a) Titration of (−)-**[ctpy-x-ctpy]** (10 μM, $CHCl_3$) with $Fe(BF_4)_2$ (0.978 mM, MeOH) followed by CD spectroscopy. The inset shows the relationship between $\Delta\epsilon$ values observed at 330 and 350 nm as a function of the equivalents of Fe(II) added (see text for details).

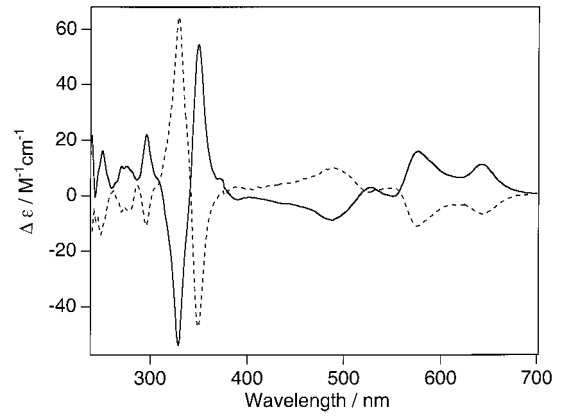

Figure 4. CD spectra of 10 μM solutions of the pure enantiomers (−)-**[ctpy-x-ctpy]** (dotted line) and (+)-**[ctpy-x-ctpy]** (solid line) in the presence of 1.5 equiv of Fe(II). Above 375 nm, the spectra were recorded for solutions 0.1 mM in ligands (see text for details).

The CD spectra of solutions of the pure enantiomers containing 1.5 equiv of Fe(II) are presented in Figure 4. As expected, a mirror image relationship of equal values but opposite sign is observed. Most prominent is the ligand-centered transition at 340 nm. Applying exciton coupling theory[17] and by comparison with related Fe(II)pinene−bipyridine triple-helical structures,[18] we assign a Δ configuration at the metal center for polymers formed by the (−)-**[ctpy-x-ctpy]** enantiomer and Λ for the (+)-**[ctpy-x-ctpy]** enantiomer, respectively. This leads to a proposed overall M helical polymeric structure for complexes formed by the (+)-**[ctpy-x-ctpy]** enantiomer and a P helical structure for those formed by (−)-**[ctpy-x-ctpy]**. The CD signals in the visible region are more difficult to interpret since they represent an overlap of transitions that are MLCT (metal-to-ligand charge transfer) and d−d in character.[14,19] We note, however, the resemblance of our results with reports in the literature for related systems.[20]

Molecular Weight Determination. Initial attempts to use gel permeation chromatography (GPC) for the determination of the degree of polymerization using THF or DMSO as eluents indicated (not surprisingly) that the behavior of the coordination polymer was not comparable to that of polymers with a purely organic backbone. The molecular weights of similar coordination polymers have been determined using 0.1 M NH_4PF_6 solutions in DMF as eluent. However, the problem of finding suitable standards remains elusive.[10,20] Attempts to determine the molecular weight of coordination polymers with vapor-phase osmometry (VPO) have also been documented in the literature, but the question of the degree of ionic dissociation in these polyelectrolytic structures, especially in apolar solvents, remains unanswerd.[21] Our attempts to determine the molecular weight with electrospray ionization mass spectrometry (ESI-MS) showed that the polymer undergoes severe fragmentation under those conditions. The main fragment detected was $[(\{(-)\text{-[ctpy-x-ctpy]}\}Fe)_n]^{2n+}$, and most other fragments were composed of the structure $[(\{(-)\text{-[ctpy-x-ctpy]}\}Fe)_n(PF_6)_m]^{(2n-m)+}$. The fragment with the largest number of $[(\{(-)\text{-[ctpy-x-ctpy]}\}Fe)_n]$ subunits found was $([(\{(-)\text{-[ctpy-x-ctpy]}\}Fe)_{8n}](PF_6)_{9n}]^{7n+})$, which establishes the presence of oligomers with at least eight Fe(II) centers. Another indication of a high degree of polymerization is the fact that a fragment with one iron center coordinated by two bridging ligand units ($[(\{(-)\text{-[ctpy-x-ctpy]}\}_2Fe)^{2+}]$) was not observed as a main fragment. Another technique to estimate the degree of polymerization is discussed in the STM section below.

STM Imaging. We recently showed that the interfacial reaction of the 2,2′:6′,2″-terpyridine-pendant dendrimers (dend-n-tpy; $n = 4$, 8, 32) and of the bridging ligand 1,4-bis[4,4″-bis(1,1-dimethylethyl)-2,2′:6′,2″-terpyridin-4′-yl]benzene (BBDTB) dissolved in CH_2Cl_2 with aqueous Fe^{2+} or Co^{2+} gives rise to ordered film formation on highly oriented pyrolytic graphite (HOPG) surfaces. The formation of the $[M(tpy)_2]^{2+}$ complexes is highly favored as both metals, Fe(II) and Co(II), have facile kinetics of complex formation and a large formation constant.[22]

STM images of (−)-**[ctpy-x-ctpy]** complexed with Fe(II) show well-ordered arrays over relatively large areas of the HOPG surface, in a way similar to our previously published work mentioned above. Figure 5 shows a 105 nm × 105 nm STM image of a (−)-**[ctpy-x-ctpy]**/Fe^{2+} film on HOPG, where the helical structure of the films is evident. As we have previously asserted, we believe that the ordered arrays consist of two-dimensional packing of 1-D strands, formed from repetitive bridging-ligand/Fe^{2+} monomers. With a typical domain size of 200−300 nm, an average polymer strand contains ca. 40−60 metal centers. This number is in good agreement with literature data reported for similar systems through gel permeation chromatography and vapor pressure osmometry.[10,20]

The question that immediately arises is whether films derived from different enantiomers can be distinguished by STM. Figure 6 shows the STM images of films derived from the reaction of each of the pure enantiomers, (+)-**[ctpy-x-ctpy]** and (−)-**[ctpy-x-ctpy]**, with Fe(II). First, it has to be pointed out that the images of both isomers are nonsuperimposable, and it is apparent that the features of the observed films are at an angle in relation to the direction of propagation. This angle is opposite for the films

(17) Ziegler, M.; von Zelewsky, A. *Coord. Chem. Rev.* **1998**, *177*, 257−300.

(18) (a) Mürner, H.-R.; Von Zelewsky, A.; Hopfgartner, G. *Inorg. Chim. Acta* **1998**, *271*, 36−39. (b) Baret, P.; Gaude, D.; Gellon, G.; Pierre, J. L. *New J. Chem.* **1997**, *21*, 1255−1257.

(19) Ferguson, J.; Herren, F.; McLaughlin, G. M. *Chem. Phys. Lett.* **1982**, *89*, 376−380.

(20) (a) Kimura, M.; Sano, M.; Muto, T.; Hanabusa, K.; Shirai, H.; Kobayashi, N. *Macromolecules* **1999**, *32*, 7951−7953. (b) Rapenne, G.; Patterson, B. T.; Sauvage, J. P.; Keene, F. R. *Chem. Commun.* **1999**, 1853−1854.

(21) (a) Nagaya, J.; Minakata, A.; Tanioka, A. *Langmuir* **1999**, *15*, 4129−4134. (b) Wandrey, C.; Zarras, P.; Vogl, O. *Acta Polym.* **1995**, *46*, 247−253.

(22) Díaz, D. J.; Storrier, G. D.; Bernhard, S.; Takada K.; Abruña.H. D. *Langmuir* **1999**, *15*, 7351−7354.

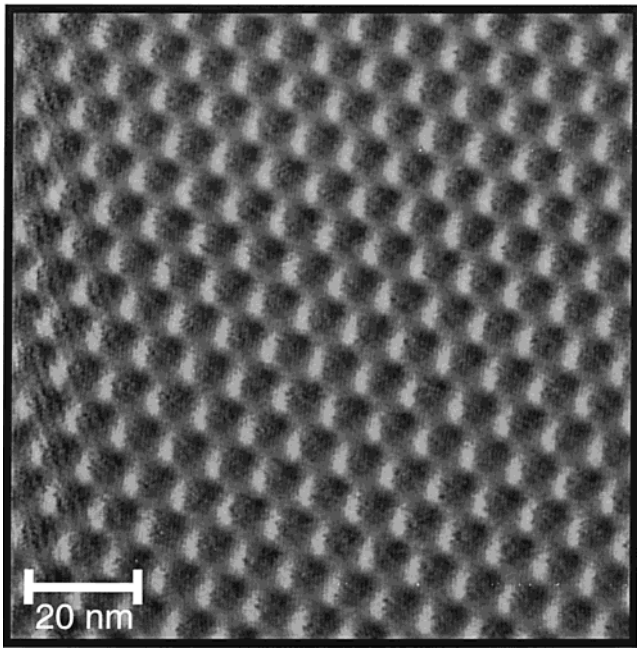

Figure 5. 105 nm × 105 nm unfiltered constant height STM image of highly ordered arrays of (−)-**[ctpy-x-ctpy]**/Fe(II) on HOPG. Scanning conditions: bias, 200 mV; setpoint current, 1.0 nA; scan rate, 10 Hz.

formed from both enantiomers, indicating that the structures formed are indeed chiral and implying a helical nature of these adsorbates. To gain a better understanding of the geometry and the handedness of these helicates, molecular mechanics calculations (MM2 force field) were performed, and the energy-minimized geometries of the bridging ligands were used to arrange bridging ligand moieties and metal centers to form helices. From this model (Figure 6) it is evident that the upper layer of the connecting bridging ligands is the origin of the angle of the features relative to the direction of propagation. Moreover, the size of these features (as derived from the STM images) is comparable to the length of the bridging ligands obtained through the MM2 optimization (3 nm). With the understanding of the structure of these organized films, it became possible to determine the absolute configuration of these helical arrangements. In agreement with the results found through the analysis of the CD spectra, it is evident from the STM images that films prepared from (+)-**[ctpy-x-ctpy]** form an M helix and that the use of the (−)-**[ctpy-x-ctpy]** stereoisomer leads to the enantiomeric P helix. It needs to be emphasized that the formation of these helical structures is only possible through the stereospecific coordination at the Fe(II) center using the enantiomerically pure bridging ligands.

Electrochemistry. Figure 7 shows a typical cyclic voltammogram for a Pt electrode in contact with a 0.10 M TBAH/AN solution containing 0.1 mM (monomer unit) of the chiral Fe polymer [((−)-**[ctpy-x-ctpy]**)−{Fe((−)-**[ctpy-x-ctpy]**)]$(PF_6)_2\}_n$. The waves, which on the initial voltammetric scan were centered at +1.02 and −1.36 V vs Ag/AgCl, correspond to metal-localized Fe(II/III) and ligand-localized processes, respectively. Although there appears to be a singular wave on the reductive sweep, we believe that the wave represents, in fact, reduction of the two terpyridine ligands bound to the metal center, as seen for $[Fe((-)\text{-ctpy})_2](PF_6)_2$.[23] The increase in current with continuous potential scanning indicates the accumulation of an

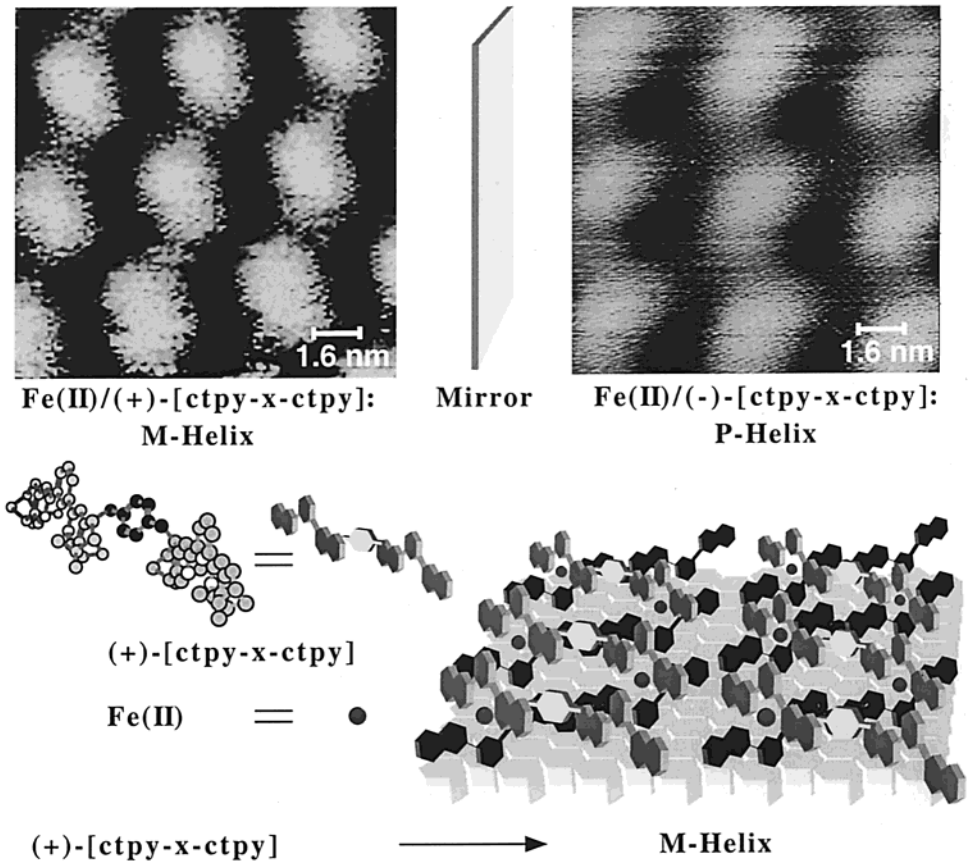

Figure 6. Top panel: High-resolution STM image of highly ordered arrays prepared from (+)-**[ctpy-x-ctpy]** or (−)-**[ctpy-x-ctpy]** and Fe(II). Bottom panel: Energy-optimized structure (MM2) of (+)-**[ctpy-x-ctpy]** (xylene spacer, black) and a rendition of the helical structure formed from this bridging ligand and Fe(II).

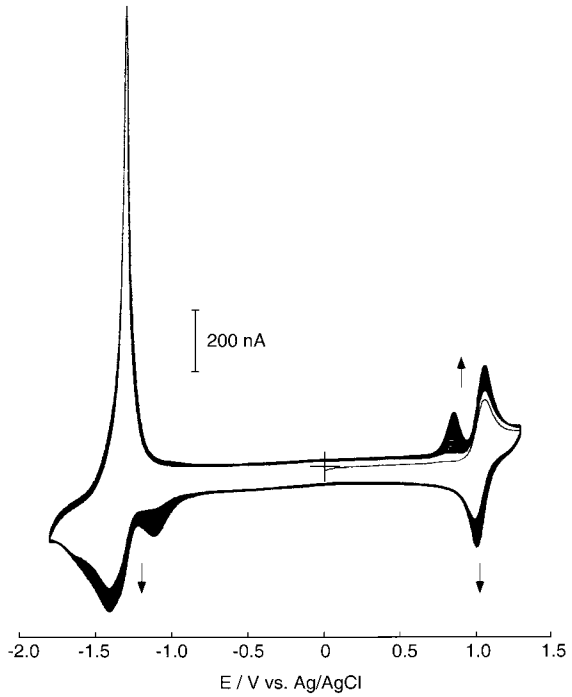

Figure 7. Typical cyclic voltammogram for a Pt electrode in contact with a 0.10 M TBAH/AN solution containing 0.1 mM (Fe unit) of ((−)-**[ctpy-x-ctpy]**)−{[Fe((−)-**[ctpy-x-ctpy]**)]$(PF_6)_2$}$_n$. Scan rate is 100 mV s^{-1}.

electroactive film on the electrode surface. The wave shape of the metal-centered process shows contributions from freely diffusing and surface-immobilized redox species. However, the anodic part of the ligand-based process (around −1.35 V) appeared to be extraordinarily sharp, even during the initial potential cycling. The full width at half-maximum (ΔE_{fwhm}) of this wave was ca. 45 mV at a sweep rate of 100 mV s^{-1}.

The cyclic voltammogram (Figure 7) also exhibits "charge-trapping peaks" at potential values of +0.85 and −1.12 V on the anodic and cathodic scans, respectively. Charge trapping is a phenomenon that was originally observed for spatially segregated bilayer redox films[24] and has since also been found in films containing two redox-active monomers[25] or a single monomer with two redox-active couples.[26] We believe that the charge-trapping peaks observed arise, at least in part, from redox centers that are electronically isolated from the surface so that their redox reactions are mediated by adjacent redox sites in a manner that is qualitatively similar to that in bilayer films.[12]

The electrodeposition of ((−)-**[ctpy-x-ctpy]**)−{[Fe((−)-**[ctpy-x-ctpy]**)]$(PF_6)_2$}$_n$ was studied in some detail using EQCM methods. The frequency response (Figure 8B) obtained concurrently with the cyclic voltammogram (Figure 8A) also supports deposition and dissolution of the polymer upon the ligand-based redox reaction. As can be clearly seen in Figure 8B, the frequency decreased during the cathodic scan from ca. −1.30 V vs Ag/AgCl, which is just prior to the ligand-centered cathodic peak potential, to −1.80 V, where the sweep direction was reversed. The frequency continued to decrease during the anodic scan to −1.40 V, and then it increased sharply and reached an approximate steady state for the remainder of the anodic scan up to +0.10 V. Further, upon continued scanning there was a gradual and continuous shift in the frequency to lower values. This suggests that when the ligands are in the reduced form, the polymer accumulates on the surface of the electrode. This may be due to low solubility of the electrically neutral polymer, as the polymer has a net zero charge after reduction of the terpyridine ligands. On the other hand, upon ligand-based oxidation, the accumulated polymer abruptly dissolved, since the polymer acquires two positive charges per redox center, resulting in an extraordinarily sharp stripping peak in the cyclic voltammogram, as mentioned earlier. A more detailed investigation of the electrochemical behavior of this redox polymer including admittance measurements of the quartz crystal resonator and studies of transport properties will be presented elsewhere.[23]

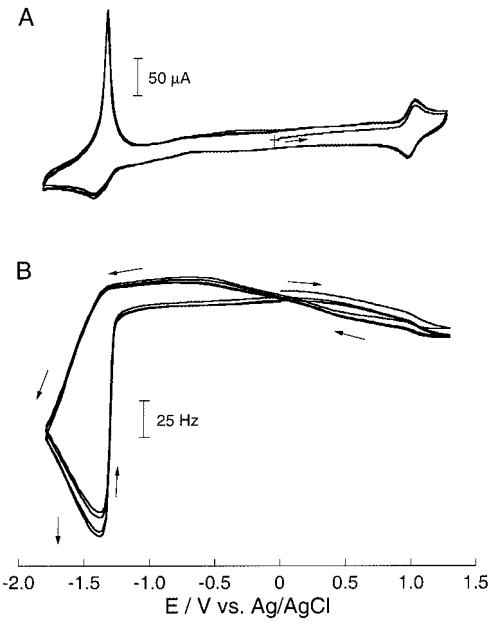

Figure 8. (A) Current (CV) and (B) frequency responses as a function of applied potential at 20 mV s^{-1} for a Pt EQCM electrode in contact with a 0.10 M TBAH/AN solution containing 0.1 mM (Fe unit) of ((−)-**[ctpy-x-ctpy]**)−{[Fe((−)-**[ctpy-x-ctpy]**)]$(PF_6)_2$}$_n$.

Conclusions

We have prepared the enantiomerically pure, bis-terpyridine-based bridging ligands (±)-**[ctpy-x-ctpy]** employing a two-fold stereospecific alkylation reaction of the enantiomerically pure, chiral terpyridyl-type ligands **(±)-ctpy**. Because of steric constraints, a single ligand molecule cannot bind to a single metal center in an octahedral fashion so that reaction of the enantiomerically pure ligands with Fe^{2+} gives rise to chiral coordination polymers whose formation and stoichiometry were followed spectrophotometrically. The absolute configuration of the formed helical polymeric structures was assigned on the basis of circular dichroism studies.

Highly ordered domains (as determined from STM imaging) of the enantiomerically pure chiral redox polymers could be prepared via the interfacial reaction, over an HOPG substrate, of the bridging ligand in CH_2Cl_2 and $FeSO_4$ in water. The STM images of the resulting films showed clear evidence of their chiral nature, and the absolute configuration of these helical structures was found to be identical to the stereochemistry of the polymers determined via circular dichroism. The degree of

(23) Takada K.; Bernhard, S.; Abruña, H. D. Manuscript in preparation.
(24) Abruña, H. D.; Denisevich, P.; Umaña, M.; Meyer, T. J.; Murray, R. W. *J. Am. Chem. Soc.* **1981**, *103*, 1−5.
(25) Guarr, T. F.; Anson, F. C. *J. Phys. Chem.* **1987**, *91*, 4037−4043.
(26) (a) Gottesfeld, S.; Redondo, A.; Rubinstein, I.; Feldberg, S. W. *J. Electroanal. Chem.* **1989**, *265*, 15−22. (b) Arana, C.; Keshavarz, M.; Potts, K. T.; Abruña, H. D. *Inorg. Chim. Acta* **1994**, *225*, 285−295. (c) Winkler, K.; Costa, D. A.; Hayashi, A.; Balch, A. L. *J. Phys. Chem. B* **1998**, *102*, 9640−9646

polymerization was estimated to be up to 60 from analysis of the STM images of the highly ordered domains on HOPG.

The electrochemical properties of the polymers were investigated using cyclic voltammetry and the electrochemical quartz crystal microbalance. Contrary to the behavior of analogous monomeric complexes, the polymeric materials undergo electrodeposition following the two-electron reduction of each bridging ligand unit (one electron per terpyridine group) and rapid stripping upon reoxidation. No such electrodeposition was observed for the metal-based oxidation.

We are currently exploring the application of these chiral interfaces to enantioselective electrosynthesis as well as to electrochromic devices. Moreover, we are also preparing redox coordination polymers with other transition metals including Ru, Co, and Os. The results of these investigations will be presented elsewhere.

Acknowledgment. D.J.D. acknowledges CCMR support through a Robert L. Sproull Fellowhsip and the Ford Foundation Fellowship. S.B. acknowledges a Fellowship for Advanced Researchers from the Swiss National Science Foundation (Grant 8220-053387). The authors thank Simon Bernhard for his help during the preparation of (−)-**ctpy**.

JA011020J